An oriented-design simplified model for the efficiency of a flat plate solar air collector

David Luna [a], Yves Jannot [b,*], Jean-Pierre Nadeau [a]

[a] Arts et Métiers ParisTech, Laboratoire TREFLE, Esplanade des Arts et Métiers, Talence Cedex, F33405, France
[b] LEMTA, Nancy Université, CNRS, 2, avenue de la Forêt de Haye 54504 Vandoeuvre, France

ARTICLE INFO

ABSTRACT

In systems design, suitably adapted physical models are required. Different modelling approaches for a solar air collector were studied in this paper. First, a classical model was produced, based on a linearization of the conservation of energy equations. Its resolution used traditional matrix methods. In order to improve the possibilities for use in design, the behaviour of the collector was next expressed in terms of efficiency. Lastly, simplified models constructed from the results obtained with the classical linearized model, and explicitly including the design variables of the collector, were proposed. These reduced models were then evaluated in terms of **P**arsimony, **E**xactness, **P**recision and **S**pecialisation (**PEPS**). It was concluded that one of them (D2), using a low number of variables and of equations, is well suited for the design of solar air collector coupled with other sub-systems in more complex devices such as solar kiln with energy storage.

© 2010 Elsevier Ltd. All rights reserved.

1. Introduction

The work presented in this article has been realized as a part of the global modelling of a solar kiln with energy storage as shown in the diagram in Fig. 1.

In order to optimise the design of a dryer like this, each constituent element must be modelled, i.e. the drying chamber, the solar collectors and the storage system (Luna et al. [1]). Nevertheless, the models of the different elements should be coherent one with another, in other words they should have the same level of exactness and precision.

Moreover, when carrying out space-temporal modelling of the drying process in the drying chamber, a resolution with a very short time interval is essential. In order to simplify programming and reduce computation time, it is interesting to look for a parsimonious model for solar collectors. A parsimonious model is a model that represents the performance of a system with a minimum number of equations and variables.

To design the system, it is essential to know the temperature of the air leaving the collector as a function of the temperature of the air entering, the time of day and the dimensions of the collector.

First a study of the available global models is done leading us to choose the linearized model that enables the calculation of the useful flux required to heat the transfer fluid.

Next the behaviour of the collector is defined by its efficiency that is the ratio between the useful heat flux transmitted to the air flow and the power received by the collector. This efficiency may be considered as a linear function of the difference between the external temperature and a reference temperature, which may be either the mean temperature of the absorber, or the entry temperature of the air.

A simplified model based on the efficiency is then presented. It expresses the efficiency as a function of the design variables of the collector and of the input air flow rate. The final model involved the system's design variables (DeV), operating variables (OpV) and auxiliary variables (AV) (Table 1). This model enables us to define the design variables for a given efficiency [2–4]. It was evaluated according to a procedure estimating the Parsimony, the Exactness, the Precision and the Specialisation of a model (PEPS method, [4]).

2. Description of the solar collector

The collector under consideration is a flat plate solar air collector consisting of a transparent cover, a blackened metal sheet (absorber) and an insulated base that delimitates an air duct. The insulation at the front consists of a layer of air trapped between the transparent cover and the absorber. Its dimensions are defined by the following design variables (DeV): length L and width l (i.e. capture surface $A_{cap} = L\,l$) and height of channel d (Fig. 2).

* Corresponding author. Tel.: +33 (0) 383595627; fax: +33 (0) 383595627.
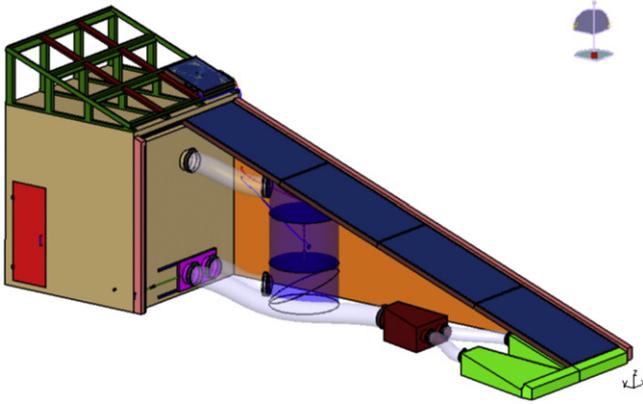E-mail address: yves.jannot@ensem.inpl-nancy.fr (Y. Jannot).

Fig. 1. Schema of the solar kiln dryer.

3. Classical model

Our aim was to obtain a system of equations enabling the evaluation of the useful flow (φ_u) recovered by the heat transfer fluid (air). The functioning of a solar collector is described by the energy conservation equations written for all the components (cover, absorber, base) and for the heat transfer fluid (air). The non-linear system thus obtained may be resolved by numerical analysis (Duffie and Beckman [5]) or, after a linearization process, by using matrix methods (Hegazy [6]). The later method was selected as it is quicker.

3.1. Energy balances

Fig. 3 shows the heat transfers that take place between the different components of the solar collector.

In a control volume, the relevant variable for each entity is its temperature (T_c, T_p, T_b, T_{a-cap}). The temperatures T_c, T_p and T_b are assumed to be uniform and permanent for a given time interval. The global model is therefore a system of 4 equations with 4 unknown parameters.

The radiative balances were written according to the methodology described by Jannot and Coulibaly [7]. The convective balances were written in the classical way for each component. It is customary to disregard the effect of the thermal inertia of these components (transparent cover, absorber, base). The lateral heat losses are neglected since the lateral area is thermally insulated and is low compared to the collector area.

3.2. Energy conservation for the transparent cover

The global balance is : $\phi_{R \to c} + \phi_{conv \to c} = 0$ (1)

The radiative balance is thus written:

$$
\phi_{R \to c} = G^* \alpha_{cs} + G^* \frac{\alpha_{cs} \tau_{cs} (1 - \alpha_{ps})}{1 - \rho_{cs}(1 - \alpha_{ps})} + \phi_{sky} \alpha_{ci}
$$
$$
+ \phi_{sky} \frac{\alpha_{ci} \tau_{ci} (1 - \alpha_{pi})}{1 - \rho_{ci}(1 - \alpha_{pi})} + \alpha_{ci} \sigma T_c^4 \frac{\alpha_{ci}(1 - \alpha_{pi})}{1 - \rho_{ci}(1 - \alpha_{pi})}
$$
$$
+ \alpha_{pi} \sigma T_p^4 \frac{\alpha_{ci}}{1 - \rho_{ci}(1 - \alpha_{pi})} - 2\alpha_{ci} \sigma T_c^4 \quad (2)
$$

The flow radiated by the sky (φ_{sky}) was determined by:

$$
\phi_{sky} = \sigma \varepsilon_a T_a^4 \quad (3)
$$

Where: ε_a is the atmospheric emissivity calculated by [8]:

Table 1
Identification of the design variables for the heating unit (solar air collector).

Function	Flow	DeV	OpV	AV
Transform solar energy into heat energy	Solar energy	L	U_a	q_a
	Heat energy	l	η	
			T_{ext}, T_{a-cap0}	
			T^*	
			G^*	

$$
\varepsilon_a = 0.787 + 0.764 \ln\left(\frac{T_{da}}{273}\right) \quad (4)
$$

Where: T_{da} corresponds to the atmosphere dew point.
The convective balance is written:

$$
\phi_{conv \to c} = -h_{p-c}(T_c - T_p) - h_{wind}(T_c - T_{ext}) \quad (5)
$$

The convective coefficient between the air and the cover is expressed by [4]:

$$
h_{wind} = 5.7 + 3.8 U_{wind} \quad (6)
$$

The calculation for the convective coefficient for exchange between the cover and the absorber (h_{p-c}) through a layer of trapped air is written:

$$
h_{p-c} = \frac{\lambda_a Nu}{e_{ac}} \quad (7)
$$

The Nusselt number (Nu) was calculated using the following equation from Daguenet [9]:

$$
Nu = \left(\frac{Gr}{Grc}\right)^{0.3} \quad (8)
$$

with :
$$
\begin{array}{ll}
Grc = 1060 & \text{if } s < 10° \\
Grc = 1060 + 0.32(s - 10)^{2.23} & \text{if } 10° < s < 70°
\end{array}
$$

where: s is the absorber tilt angle

3.3. Energy conservation for the absorber

The global balance is : $\phi_{R \to p} + \phi_{conv \to p} = 0$ (9)

The radiative balance is:

$$
\phi_{R \to p} = G^* \frac{\alpha_{ps} \tau_{cs}}{1 - \rho_{cs}(1 - \alpha_{ps})} + \phi_{sky} \frac{\alpha_{ci} \tau_{ci}}{1 - \rho_{ci}(1 - \alpha_{pi})}
$$
$$
+ \alpha_{ci} \sigma T_c^4 \frac{\alpha_{pi}}{1 - \rho_{ci}(1 - \alpha_{pi})} + \alpha_{pi} \sigma T_p^4 \frac{\alpha_{ci} \rho_{ci}}{1 - \rho_{ci}(1 - \alpha_{pi})}
$$
$$
- \sigma \frac{T_p^4 - T_b^4}{\frac{1}{\alpha_{pi}} + \frac{1}{\alpha_{bi}} - 1} - \alpha_{pi} \sigma T_p^4 \quad (10)
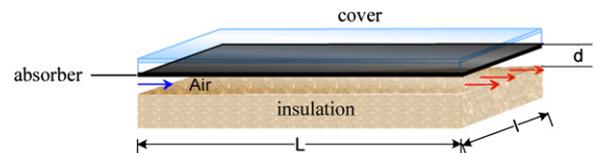$$

Fig. 2. Design variables (DeV) of the solar air heater.

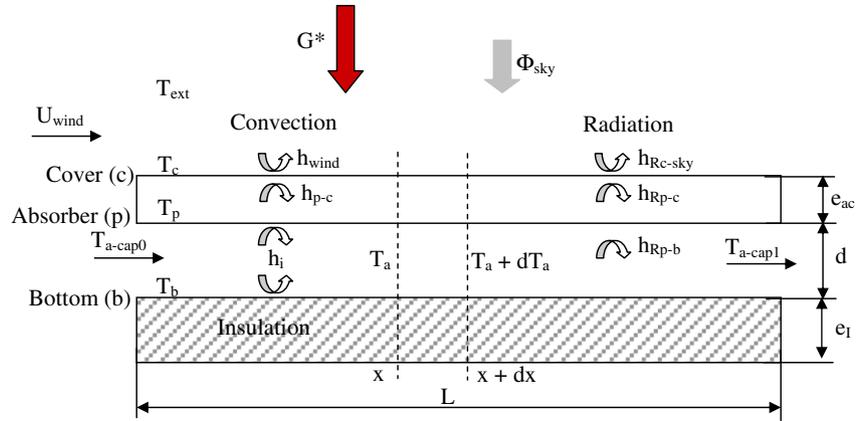**Fig. 3.** Heat exchanges in the solar air heater.

The convective balance is:

$$\phi_{\text{conv}\to\text{p}} = -h_{\text{p-c}}A_{\text{p}}(T_{\text{p}} - T_{\text{c}}) - \frac{h_{\text{i}}A_{\text{p}}}{2}(T_{\text{p}} - T_{\text{b}})\frac{q_{\text{a}}\text{Cp}_{\text{a}}}{2}$$
$$\times \left[\frac{T_{\text{p}} + T_{\text{b}}}{2} - T_{\text{a-cap0}}\right]\left[1 - \exp\left(\frac{-2h_{\text{i}}A_{\text{p}}}{q\text{Cp}_{\text{a}}}\right)\right] \quad (11)$$

h_{i}: the convective coefficient for exchange between the absorber and the air and between the base and the air is calculated using the following equation (Holman, [10]):

$$h_{\text{i}} = \frac{\lambda_{\text{a}}}{d}0.023\text{Re}^{0.8}\text{Pr}^{0.3} \quad (12)$$

3.4. Energy conservation for the base

The global balance is : $\phi_{\text{R}\to\text{b}} + \phi_{\text{conv}\to\text{b-a}} + \phi_{\text{cond}\to\text{b-ext}} = 0$ (13)

The radiative balance is written thus:

$$\phi_{\text{R}\to\text{b}} = \sigma\frac{T_{\text{p}}^4 - T_{\text{b}}^4}{\frac{1}{\alpha_{\text{pi}}} + \frac{1}{\alpha_{\text{bi}}} - 1}A_{\text{b}} \quad (14)$$

The convective balances are:

$$\phi_{\text{conv}\to\text{b-a}} = \frac{h_{\text{i}}A_{\text{b}}}{2}(T_{\text{b}} - T_{\text{p}})\frac{q_{\text{a}}\text{Cp}_{\text{a}}}{2}\left[\frac{T_{\text{p}} + T_{\text{b}}}{2} - T_{\text{a-cap0}}\right]\left[1\right.$$
$$\left. - \exp\left(\frac{-2h_{\text{i}}A_{\text{b}}}{q\text{Cp}_{\text{a}}}\right)\right] \quad (15)$$

$$\phi_{\text{cond}\to\text{b-ext}} = \frac{T_{\text{b}} - T_{\text{ext}}}{\frac{e_{\text{I}}}{\lambda_{\text{I}}A_{\text{b}}}} \quad (16)$$

3.5. Energy conservation for the air

The energy balance for the air is : $h_{\text{i}}(2T_{\text{a}} - T_{\text{b}} - T_{\text{p}})l\text{dx} - q\text{Cp}_{\text{a}}\text{d}T_{\text{a}}$
$= 0$
(17)

By integration, useful flow is expressed by the relation:

$$\phi_{\text{u}} = q\text{Cp}_{\text{a}}(T_{\text{a-cap1}} - T_{\text{a-cap0}})$$
$$= q\text{Cp}_{\text{a}}\left(\frac{T_{\text{p}} + T_{\text{b}}}{2} - T_{\text{a-cap0}}\right)\left[1 - \exp\left(\frac{-2h_{\text{i}}A_{\text{cap}}}{q\text{Cp}_{\text{a}}}\right)\right] \quad (18)$$

3.6. Linearizing the energy balances

A change of variables has been done to linearize the equations of the energy balances, the new variables are: $(T_{\text{p}}-T_{\text{ext}})$, $(T_{\text{c}}-T_{\text{ext}})$, $(T_{\text{b}}-T_{\text{ext}})$, and $(T_{\text{a-cap1}}-T_{\text{ext}})$. As an example, the third term of relation (10) may be written as:

$$\alpha_{\text{ci}}\sigma T_{\text{c}}^4\frac{\alpha_{\text{pi}}}{1 - \rho_{\text{ci}}(1 - \alpha_{\text{pi}})} = h_1(T_{\text{c}} - T_{\text{ext}}) + C_1 \quad (19)$$

With : $h_1 = \frac{\sigma\alpha_{\text{ci}}\alpha_{\text{pi}}}{1 - \rho_{\text{ci}}(1 - \alpha_{\text{pi}})}\left(T_{\text{c}}^2 + T_{\text{ext}}^2\right)(T_{\text{c}} + T_{\text{ext}})$ (20)

And : $C_1 = \frac{\sigma\alpha_{\text{ci}}\alpha_{\text{pi}}}{1 - \rho_{\text{ci}}(1 - \alpha_{\text{pi}})}T_{\text{ext}}^4$ (21)

The coefficient h_1 weakly varies if T_{c} varies by several degrees, thus it and may be calculated with an approximate value of T_{c} and then considered as a constant. Processing in the same manner all the terms of the relations resulting from the energy balances leads to a linear system of four equations with four unknown variables $(T_{\text{p}}-T_{\text{ext}})$, $(T_{\text{c}}-T_{\text{ext}})$, $(T_{\text{b}}-T_{\text{ext}})$, and $(T_{\text{a-cap1}}-T_{\text{ext}})$.

The system is resolved using a matrix method and in this way the evolution of T_{p}, T_{c}, T_{b} and T_{a} can be calculated.

This classical code is fairly cumbersome to implement with meteorological data and air entry conditions that vary continuously over a long period; it is not easy to combine it with the simulation code for drying in the drying chamber. It is the reason why a reduced model has been established, it that will now be described.

3.7. Efficiency of a solar collector

Efficiency relates to the performance of thermal systems, it is traditionally used to define heat exchangers and is expressed as the ratio of recovered power to maximum recoverable power. It depends on the system design but also on operating and external conditions.

The efficiency is the measurement of the performance of a collector, defined as the ratio of energy achieved to incident solar energy for the same period of time (Duffie and Beckman [5]). This mean efficiency is calculated as:

$$\eta = \frac{\int \phi_{\text{u}}\text{dt}}{A_{\text{cap}}\int G^*\text{dt}} \quad (22)$$

Using the global energy balance of the solar collector as a departure point, the instantaneous efficiency was defined as the ratio of the power recovered by the collector to the incident solar flow, thus:

$$\eta = \frac{\phi_s - \phi_\rho - \phi_P}{\phi_s} = \frac{\phi_u}{G^* A_{cap}} = \frac{q_a Cp_a (T_{a-cap1} - T_{a-cap0})}{G^* A_{cap}} \quad (23)$$

Efficiency must now be expressed as a function of the relevant design parameters, operational variables (air flow rate and air temperatures) and external conditions.

3.8. Expressing efficiency according to temperature of the absorber

Duffie and Beckman [5] suggest using the absorber as a reference to evaluate transfers into the collector and losses towards the exterior. Thus the net solar flow recovered by the absorber can be expressed in the following form:

$$\phi_s - \phi_\rho = \tau_c \alpha_p G^* A_{cap} \quad (24)$$

Losses can then be written based on the temperature T_p of the absorber:

$$\phi_P = hp A_{cap} (T_p - T_{ext}) = \phi_{av} + \phi_{ar} \quad (25)$$

Heat losses at the front (av) and back (ar) take into account convective and radiative exchanges and also conduction (in the insulating material). Considering the type of collector studied, hp can be expressed with the following equation (Duffie and Beckman [5]):

$$hp = \cfrac{1}{\cfrac{1}{\cfrac{1}{h_{c,p-c} + h_{R,p-c}} + \cfrac{1}{h_{wind} + h_{R,c-ext}}} + \cfrac{1}{\cfrac{1}{h_{c,p-b} + h_{R,p-b}} + \cfrac{e_I}{\lambda_I} + \cfrac{1}{h_{wind}}}} \quad (26)$$

Instantaneous efficiency can now be expressed as:

$$\eta = (\tau_c \alpha_p) - hp \frac{(T_p - T_{ext})}{G^*} \quad (27)$$

The transmission τ_c and absorption α_p coefficients are constant if the transparent cover and the absorber are isothermal, the hp coefficient depends on the types of transfer and the mean value of the temperature of the absorber. As an initial approximation and at a permanent operating speed, we can say that efficiency varies in a linear fashion as a function of the expression $T^* = (T_p - T_{ext})/G^*$. Instantaneous efficiency is then expressed by equation (28):

$$\eta = B - KT* \quad (28)$$

The values $B(B = \tau_c \alpha_p)$ and $K(K = hp)$ are called, respectively, the optical factor of the collector and the total thermal conductance of the losses.

When the collector is assumed to be at a permanent operating speed, and the cover and absorber are isothermal, then the optical factor $B = \tau_c \alpha_p$ and the conductance $K(K = hp)$ are constant. Within these conditions, the instantaneous efficiency as a function of T^* follows a straight line (Fig. 4).

This expression is unsatisfactory for two reasons, firstly, coefficients B and K are variable as they depend on the variable operational conditions (meteorological conditions in particular) and secondly, the temperature of the absorber is only an auxiliary variable in the desired model.
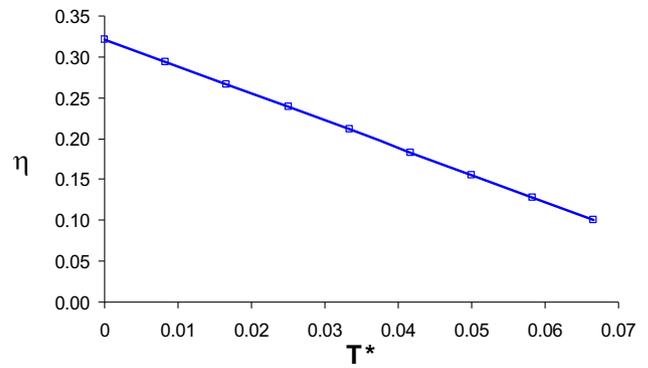

Fig. 4. Straight line efficiency of the solar air heater ($L = 10$ m, $l = 3$ m).

3.9. Expressing efficiency according to the entry temperature of the heat transfer fluid

In reality, convective and radiative heat transfers depend on actual temperatures inside the collector, in particular the air temperature, which varies.

Duffie and Beckman [5] suggest weighting the equation for the useful flux with a coefficient F_R that incorporates this variation. The temperature deviation used is then $T_{a-cap0} - T_{ext}$.

The flux is then calculated by:

$$\phi_u = A_{cap} F_R [\phi_s - hp (T_{a-cap0} - T_{ext})] \quad (29)$$

The coefficient F_R, called the conductance factor of the absorber, is obtained by integrating transfers along the length of the collector and is expressed by:

$$F_R = \frac{q_{cap} Cp}{A_{cap} hp} \left[1 - \exp \left(\frac{A_{cap} hp F'}{q_{cap} Cp} \right) \right] \quad (30)$$

This introduces a factor relating to the efficiency of the absorbent plate F', which is the ratio of heat resistance to transfers between the plate and the exterior to heat resistance to transfer between the fluid and the exterior. This factor depends on the type of collector used; its value is less than or equal to one. For the type of collector studied here, F' is given in the following expression:

$$F' = \cfrac{1}{1 + \cfrac{hp}{h_i + \cfrac{1}{\cfrac{1}{h_i} + \cfrac{1}{h_{R,p \to b}}}}} \quad (31)$$

Thus instantaneous efficiency is written:

$$\eta = F_R \left[(\tau_c \alpha_p) - hp \frac{(T_{a-cap0} - T_{ext})}{G^*} \right] \quad (32)$$

$F_R(\tau_c \alpha_p)$ and $F_R hp$ are two parameters that correctly describe the functioning of a collector.

Efficiency as a function of $(T_{a-cap0} - T_{ext})/G^*$ is represented by a straight line with a negative slope $F_R hp$ and an intercept point $F_R \tau_c \alpha_p$, as shown in Fig. 5. Nevertheless, in reality h_p varies (weakly) with the temperature at which the collector is operational and with climatic conditions. In fact, the true curve deviates from the theoretical straight line for higher values of T^* (Mathioulakis et al. [11]).

The expression of efficiency η (relation (32)) introduces the true functioning of the collector via factor F_R. With this factor, we take into account the changes in the temperature of the fluid (T_a) and of the absorber (T_p) and also the changes in heat transfers between absorber and fluid (F').
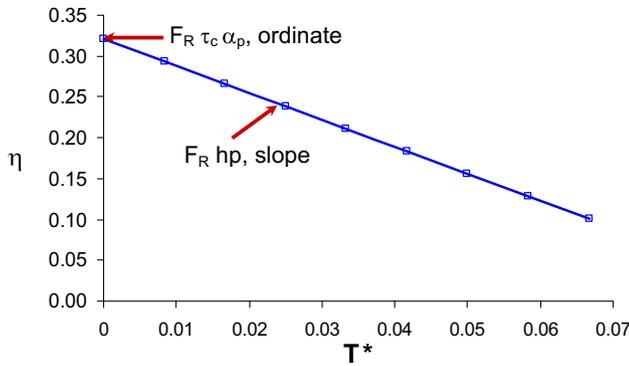
Fig. 5. Instantaneous efficiency of the solar air heater, a function of T*.

4. Parsimonious models for design

In the previous efficiency models, the design variables did not intervene explicitly. In order to optimise system design, it is interesting to express efficiency as a function of design variables L and l and of the operational system variable, i.e. air flow rate q_a. The third design variable, the height of the air channel, was fixed at $d = 50$ mm.

The variables that are relevant to changes in efficiency are the Design Variables L and l and the Operating Variable q_a (Table 1).

The auxiliary variable U_a (air velocity) is a variable that enables the behaviour of the air in the collector to be analysed in terms of fluid mechanics (Reynolds number, Re). Internal transfers between the absorber and the heat transfer fluid also vary with U_a that is directly linked with the design variable l and the operational variable q_a, thus:

$$U_a = \frac{q_a}{dl} \tag{33}$$

An expression of the efficiency as a function of L and U_a is proposed, it is based on results obtained from a numerical experimental design using the traditional simulation code.

The desired equation takes the form:

$$\eta = B(L, U_a) - K(L, U_a)T^* \tag{34}$$

The function $f(L,U_a)$ represents the deviation of the true curve from a mean straight line when T_p and T_{ext} varies.

The results of the simulations represented on Fig. 6 highlights the dependence of the efficiency to L and U_a through the variations of B and K. Fig. 6 shows that B and $(-K)$ varies in the same way and rather proportionally. As expected, the efficiency increases when U_a increases since the heat transfer convective coefficient between air

and the collector increases. It may also be seen that the efficiency decreases when the collector length increases. It may be explained by the increasing of the mean value T_p leading to a decreasing of the efficiency as expressed by relation (27).

These results enabled us to carry out a parametric study on the values of B and K as a function of the relevant variables L and U_a that have a variation range of:

$$5 < L < 25\text{m and } 1.39 < U_a < 4.17\text{m·s}^{-1}$$

It has been verified that a variation of the height of the channel d between 20 mm and 100 mm has no significant influence of the values of B and K when U_a varies between 1.39 and 4.17 m s^{-1}.

To calculate T* ($T^* = (T_{a-cap0} - T_{ext})/G^*$), the temperature T_{ext} was fixed at 30 °C and the temperature T_{a-cap0} varied according to the temperatures measured at the input to the collector (20°C < T_{a-cap0} < 60 °C). The value of G^* was constant and fixed at 600 W m^{-2}. For verifying that the choice of the values of T_{ext} and G^* have no influence on the results, other efficiency calculations have been done with $T_{ext} = 20$ °C, and $G^* = 300$ and 900 W m^{-2}. They lead to the same results for a given value a T^*.

4.1. First data analysis: model D1

A first simplified model D1 was studied under the form:

$$\eta = (B_o - K_o T^*)f(L, U_a) \tag{35}$$

with: $B_o = \tau_c \alpha_p$ and K_0 chosen as a mean value of hp.

The function $f(L,U_a)$ represents the deviation of the true curve from a mean straight line when T_p and T_{ext} varies. The value of $\tau_c \alpha_p$ was fixed at 0.81 in agreement with the optical properties of the transparent cover and the absorber. Numerical simulations were used to calculate hp and the efficiency η for values of L and U_a varying inside the previously defined intervals. It was found that hp varies from 8.17 to 8.52 W m^{-2} K^{-1}, with a mean value of 8.34 W m^{-2} K^{-1}, so that the following values were retained for relation (34): $B_0 = 0.81$ and $K_0 = 8.34$ W m^{-2} K^{-1}.

Numerical calculation leads to the following parsimonious model D1 that can be used to calculate the instantaneous efficiency of the collector as a function of air velocity U_a and length L:

$$\eta = [0.81 - 8.34T^*][0.1649\ln U_a + 0.3948][$$
$$\times (0.0037U_a - 0.0254)L + 1.1036 - 0.0134U_a] \tag{36}$$

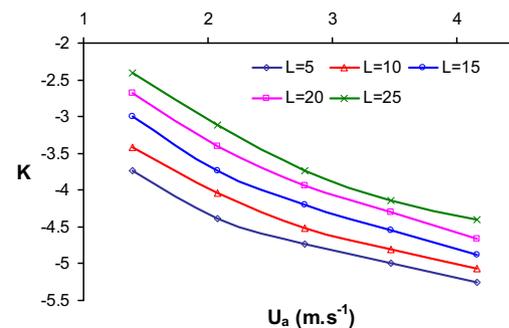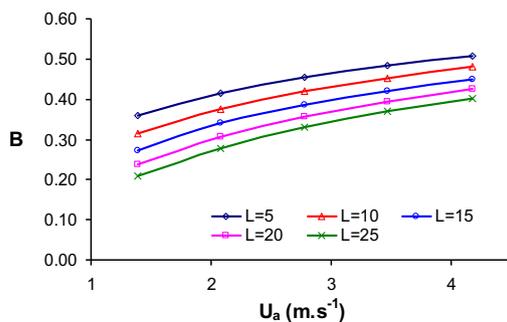$$\text{Where}: T^* = \frac{T_{a-cap0} - T_{ext}}{G^*} \tag{37}$$

Fig. 6. B and K parameter variation, a function of L and air velocity U_a.

4.2. Second data analysis: model D2

To improve the precision of the calculation of the efficiency η, a second model was studied under the form of relation (34).

Using the same data analysis for B and K, the following parsimonious model was obtained:

$$B = (0.1349\ln U_a + 0.3163)[(0.0037U_a - 0.0254)L + 1.1036 - 0.0134U_a] \tag{38}$$

$$K = (1.3613\ln U_a + 3.3291)[(0.0037U_a - 0.0226)L + 1.1086 - 0.0165U_a] \tag{39}$$

The efficiency of the collector is thus defined as:

$$\eta = [(0.1349\ln U_a + 0.3163) - (1.3613\ln U_a + 3.3291)T^*] \\ \times [(0.0037U_a - 0.0254)L + 1.1036 - 0.0134U_a] \tag{40}$$

5. Evaluation of parsimonious models

The reference model (classical model) and the parsimonious models D1 and D2 were evaluated using the PEPS method consisting in the evaluation of the parsimony, the exactness, the precision and the specialisation of a model. This method revealed the physical behaviour of the system, in order to estimate the degree of confidence that the designer can place in the results of the representation obtained from the models [2]. **Parsimony** is the parameter that defines the ability of a model to describe the physical behaviour of the system it represents with a minimum number of equations and variables. **Exactness** represents the difference between the solution space of the model and the behaviour of a reference model. The **Precision** of a model can be defined as the range in a domain of possible values for a given variable. Precision must therefore not be confused with exactness, since it measures the precision with which the result is determined, with no link to a reference value. The **Specialisation** of a model is all the hypotheses and information that limit the area of application. Depending on the system level at which one is placed and taking the restrictive hypotheses into account, a model is specialised to a greater or lesser degree.

5.1. Evaluation of parsimony

The efficiency model takes into account all variables and equations relating to the functioning of the collector. The various transfers between the absorber, the fluid and the exterior are taken into account, both with the design and operational variables of the collector. Models D1 and D2 are represented by:

− 9 variables (cf. Table 1)
− 2 equations (36), (37) or (40)

Compared with the classical model, our model was constructed with nine variables and only two explicit relations. It is therefore a very parsimonious model.

5.2. Evaluation of exactness

The efficiencies of a collector calculated using parsimonious models D1 and D2 were compared to the efficiencies calculated using the classical model considered as a reference. Fig. 7 presents the evolution of the efficiency as a function of $T^* = (T_{a-cap0} - T_{ext})/G^*$, for an air velocity of 1.39 m s^{-1}.
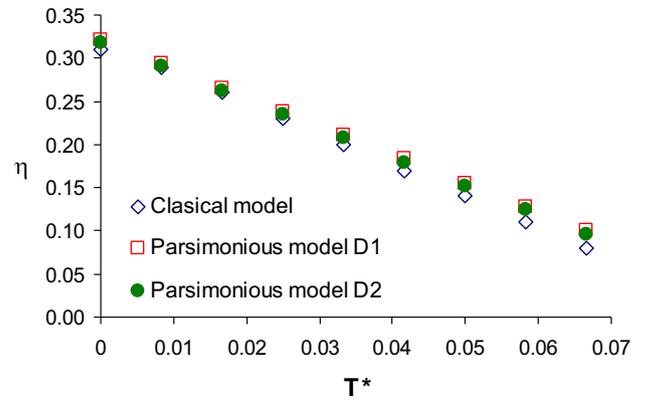

Fig. 7. Exactness models, D1 and D2 ($U_a = 1.39$ m s^{-1}).

We observed very similar behaviour between the parsimonious models and the classical model, with model D2 being more exact. The deviations calculated for model D2 were less than 3%, and we therefore concluded that this model had a high level of exactness for a range of air velocities of $1.39 < U_a < 4.17$ m s^{-1}.

5.3. Evaluation of precision

When considering the definition of precision, air velocity U_a was identified as a variable that could be a source of imprecision. An uncertainty of ± 0.1 m s^{-1} was considered for the air velocity U_a to assess the precision of the reference and to evaluate model D2. From this analysis, it was possible to identify the efficiency variation interval for each model when there is a variation in air velocity. Fig. 8 shows the variation in efficiency as a function of T^* for a low air velocity. This demonstrates more clearly the size of the interval for variations in η.

It can be noticed that the interval for possible efficiency values was smaller in the case of the parsimonious model D2. On the other hand, for the classical model, the variation range for η was greater, and the model was therefore more sensitive to variations in U_a. As a result, we affirmed that the parsimonious model was more precise than the classical model.

Model D2 was therefore considered to be exact and precise.

5.4. Evaluation of the level of specialisation

The specialisation of a model depends on its system level and on the hypotheses on which it is based. Moreover, the validity domains
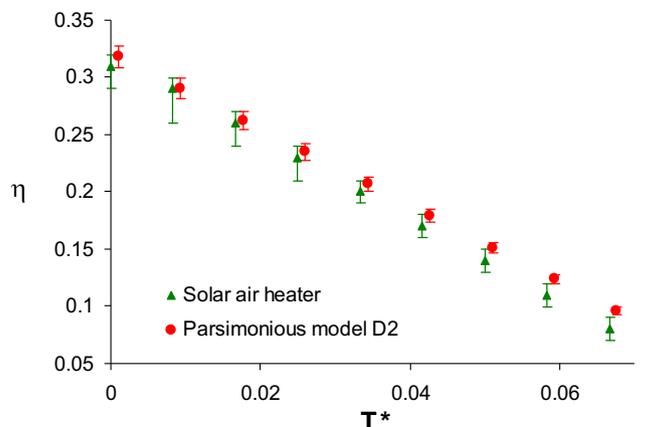

Fig. 8. Solar air heater precision valuation ($U_a = 1.39 \pm 0.1$ m s^{-1}).

Parsimony Low →→→ Strong
Exactness Low →→→ Strong
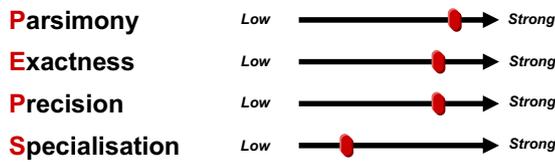**Precision** Low →→→ Strong
Specialisation Low →→→ Strong

Fig. 9. Parsimonious model D2, representation of PEPS.

according to the relevant variables for L and U_a must be analyzed; the domains were the same for the three models i.e. $5 < L < 25$ m and $1.39 < U_a < 4.17$ m s^{-1}, however, the parsimonious models were constructed with the value of d fixed at 50 mm, whereas with the classical model a variable height was possible for channel d. Models D1 and D2 are therefore more specialised.

The models used to describe the behaviour of the solar air collector were evaluated on the basis of the four PEPS parameters. The result is that the model D2 is very parsimonious, more exact than model D1 when compared with the classical model, very precise, especially for high air velocity values and fairly specialised as the variable "d" was fixed. Evaluation of these parameters is summarised in Fig. 9.

6. Conclusion

Using computations from the very first phases of the design process requires specific and dedicated models for this phase.

A global model based on the laws of energy conservation was first established. This model was linearized so that it could be processed using matrix methods. It was then used as a reference in order to validate simplified models.

The study was based on the concept of efficiency and enabled us to define equations based on reduced expressions in order to validate parsimonious models based on the design variables of a solar air collector. Two simplified models were constructed from the parametrized results obtained with the linearized global model.

Analysis of these models was based on 4 properties: their parsimony, their exactness compared with a classical global model used as a reference, their precision and their specialisation. Reduced model D2 showed practically the same qualities as the classical model but with a higher parsimony. It is thus well suited for the design of solar air collector coupled with other sub-systems in more complex devices such as solar kiln with energy storage as done by Luna [12].

Nomenclature

A	Exchange surface (m^2)
Cp	Specific heat (J kg^{-1} K^{-1})
d	Height of channel in collector (m)
dh	Hydraulic diameter (m)
e	Thickness (m)
F'	Collector efficiency factor
FR	Conductance factor of the absorber
G*	Solar heat flux density (W m^{-2})
h	Convective exchange coefficient (W m^{-2} K^{-1})
hp	Global loss coefficient (W m^{-2} K^{-1})

L	Length (m)
l	Width (m)
q	Air mass flow (kg s^{-1})
T	Temperature (°C)
s	Absorber tilt angle (°)
t	Time (s)
U	Velocity (m s^{-1})
α	Absorptivity
ϕ	Heat Flow (W m^{-2})
λ	Thermal conductivity (W m^{-1} K^{-1})
η	Collector efficiency
ε	Emissivity

Subscripts

0	Entry
1	Exit
a	Air
b	Base
c	Cover
cap	Collector
cond	Conduction
conv	Convection
ext	Exterior
i	Infrared
I	Insulating material
P	Lost flow
p	absorber
r	Reflected flow
R	Radiation
s	Solar radiation

References

[1] D. Luna, J.P. Nadeau, Y. Jannot, Solar timber kilns: state of the art and foreseeable developments, Renewable and Sustainable Energy Reviews 13 (6–7) (2009) 1446–1455 2008 Elsevier, Oxford, England.

[2] J. Pailhes, M. Sallaou, J.P. Nadeau, Knowledge base formulation for aided design tool. in: Serge Tichkiewitch, Michel Tollenaere, Pascal Ray (Eds.), Trends and Recent Advances in Integrated Design and Manufacturing in Mechanical Engineering II. Springer Verlag, 2007, pp. 231–243.

[3] D. Scaravetti, J. Pailhes, J.P. Nadeau, P. Sebastian, Aided decision-making for an embodiment design problem. in: A. Bramley, D. Brissaud, D. Coutellier, C. McMahon (Eds.), Advances in Integrated Design and Manufacturing in Mechanical Engineering. Springer, Dordrecht, 2005, pp. 159–172.

[4] Y. Vernat, J.P. Nadeau, P. Sebastian, Formalisation and qualification of models adapted to preliminary design, International Journal Interactive Design and Manufacturing 4 (2010) 11–24.

[5] J.A. Duffie, W.A. Beckman, Solar Engineering of Thermal Processes, third ed. John Wiley and Sons, Inc, New Jersey, 2006.

[6] A.A. Hegazy, Optimizing the thermohydraulic performance of flat-plate solar air heaters operating with fixed/variable pumping power, Renewable Energy 18 (1999) 283–304.

[7] Y. Jannot, Y. Coulibaly, Radiative heat transfer in a solar air heater covered with a plastic film, Solar Energy 60 (1) (1997) 35–40.

[8] G. Clark, C.P. Allen 1978, The estimation of atmospheric radiation for clear and cloudy skies, Proceedings of the second national passive solar conference, Philadelphia, Part.2, p.676.

[9] M. Daguenet, Les Séchoirs Solaires: Théorie et Pratique. UNESCO, 1985.

[10] J.P. Holman, Heat Transfer, seventh ed. Mac Graw Hill, 1990, p.284.

[11] E. Mathioulakis, K. Voropoulos, V. Belessiotis, Assessment of uncertainty in solar collector modeling and testing, Solar Energy 66 (5) (1999) 337–347.

[12] D. Luna, Modélisation et conception préliminaire d'un séchoir solaire pour bois de pin avec stockage d'énergie. Thèse doctorat, Arts et Métiers Paris Tech., 2008.